ACCOUNTS
of chemical research

Functional Hybrid Systems Based on Large-Area High-Quality Graphene

JOHANN CORAUX,* LAËTITIA MARTY, NEDJMA BENDIAB, AND VINCENT BOUCHIAT

Institut NÉEL, CNRS & Université Joseph Fourier, BP166, F-38042 Grenoble Cedex 9, France

RECEIVED ON MAY 19, 2012

CONSPECTUS

The properties of sp^2 carbon allotropes can be tuned and enriched by their interaction with other materials. The large interface to the outside world in these forms of carbon is ideally suited for combining in an optimal manner several functionalities thanks to this interaction. A wide range of novel materials holding strong promise in energy, optoelectronics, microelectronics, mechanics, or medical applications have been designed accordingly. Graphene, the last representative of this family of sp^2 carbon materials, has already yielded a wealth of hybrid systems. A new class of these hybrids is emerging, which allows researchers to exploit the properties of truly single-layer graphene. These systems rely on high-quality graphene.

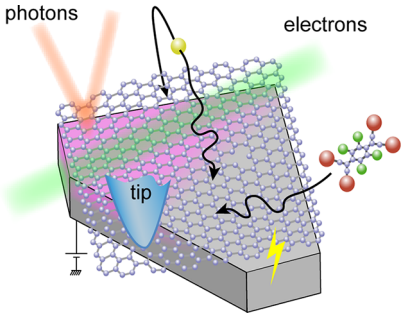

In this Account, we describe our recent efforts to develop hybrid systems through various approaches and with various scopes. Depending on the interaction between graphene and molecules, metal clusters, layers, and substrates, either graphene may essentially preserve the electronic properties that make it a unique platform for electronic transport, or new organization and properties in the materials may arise due to the graphene contact at the expense of deep modification of graphene's properties. We prepare our graphene samples by both mechanical exfoliation of graphite and chemical vapor deposition on metals. We use this to study graphene in contact with various species, which either decorate graphene or are intercalated between it and its substrate. We first address the electronic and magnetic properties in systems where graphene is in epitaxy with a metal and discuss the potential to manipulate the properties of both materials, highlighting graphene's role as a protective capping layer in magnetic functional systems. We then present graphene/metal dot hybrids, which can utilize the two-dimensional gas properties of Dirac fermions in graphene. These hybrids allow one to tune the coupling between clusters hosting electronically ordered states such as superconductivity and explore quantum phase transitions controlled by electrostatic back gates. We finally discuss the optical properties of hybrids in which graphene is decorated with optically active molecules. Depending on how close these molecules are to the graphene's electromechanical systems, the interaction of the system with light can be changed. Fields such as spintronics and catalysis could benefit from high-quality graphene based hybrid systems, which have not been fully explored.

1. Introduction

The term "hybrid" has become common since its use in automotive industry. It is employed in various areas of science, for instance, in genetics when referring to the offspring of animals or plants belonging to different species. The synthesis and chemistry of hybrid molecules or supramolecular networks goes well beyond the notion of strong bonding of functional groups of atoms through atomic orbital hybridization. Hybrid systems combine materials of different nature, like composite materials, but unlike in the latter the constituents are usually bound by some interaction, be it strong, for example, covalent-like, as in organometallic molecules and organic-modified silicates,[1] or weak, as in some layered materials intercalated with polymers.[2] The concept of the hybrid system extends to situations in which despite the absence of a bond between the compounds, at least one of the compound's properties influences those of the other compounds leading to combined or novel functions. This broad definition of a hybrid system encompasses systems whose properties are governed by proximity effects, for example, proximity-induced superconductivity.

Published on the Web 11/29/2012 www.pubs.acs.org/accounts
10.1021/ar3001519

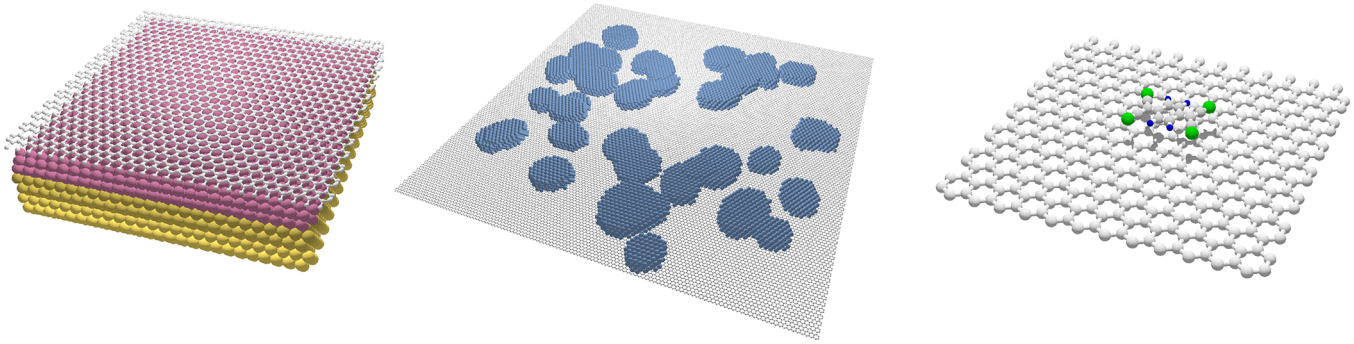

FIGURE 1. Schematics of an epitaxial graphene–metal hybrid consisting of a thin functional metal film sandwiched between a substrate and graphene (left), a graphene–metal dot hybrid (center), and a graphene–molecule hybrid (right).

A popular illustration of a hybrid system based on sp^2-carbon is found in rechargeable batteries, which rely on the reversible intercalation of Li ions in graphite electrodes.[3] In this system and many other sp^2-carbon ones, for instance, nanotubes or nanoparticles,[4] interface atoms are a strong, if not the main, fraction of the constituents of the hybrid system. This is a general characteristics of hybrid materials based on sp^2-carbon resulting from the topography of these forms of carbon. This is an attractive feature since in many cases, the extent to which the hybrid system's properties can be engineered is related to the role of interfaces.

Most systems referred to as graphene-based hybrids are prepared following chemical routes. Reports for such systems became more abundant in the past few years. Graphene may be functionalized with molecules, such as porphyrins, yielding efficient optical limiting properties,[5] that is, lower transmittance for higher-intensity light, a desirable property for protecting sensitive sensors. Graphene was also combined with a number of nanoparticles. Superparamagnetic Fe_3O_4 nanoparticle–graphene hybrids appeared well-suited for drug delivery owing to the easy magnetic field manipulation and dispersion in solutions.[6] Dealing with energy applications, the high specific surface area of graphene and its high conductivity were combined for interconnecting TiO_2 nanoparticles hosting Li during the operation of batteries.[7] Synergetic chemical coupling was unveiled in Co_3O_4 nanoparticle–graphene hybrids, leading to efficient catalytic activity for oxygen reduction, together with remarkable stability and durability.[8] These examples all rely on graphene randomly structured at the nanoscale due to the preparation method, either the reduction or the thermal expansion of graphene oxide. Besides their ill-defined topography, these graphenes also have a large density of defects, such as epoxy or hydroxy groups left after the reduction step.

The term "hybrid" recently also was employed for systems composed of high-quality graphene, produced by exfoliating graphite or epitaxial growth on metallic or silicon carbide substrates. Very schematically, such samples are developed in the view of electronic transport, surface science studies, or both. Our group studies a variety of systems, including exfoliated and epitaxial graphene decorated with nanoparticles or molecules and in contract with ultrathin magnetic layers. With the view of efficient electronic transport, weak bonding between graphene and the material it is in contact with is preferred. A somewhat opposite situation is that of graphene deposited onto another material for manipulating its properties. In this, the intrinsic properties of graphene, for instance, its transport properties, may be strongly affected.

In this Account, we address epitaxial graphene–metal hybrids, graphene–metal dot hybrids, and graphene–molecule hybrids (Figure 1). We present our recent work in these directions and put it in light of the literature. We show how such hybrids allow us to achieve novel functionalities in graphene and in the materials with which it is in contact.

2. Electronic and Magnetic Properties in Epitaxial Graphene/Metal Hybrids

A simple epitaxial graphene–metal hybrid is graphene on its metallic substrate. Graphene strongly interacts with substrates like Ni, Co, Rh, Re, Pd, or Ru[9] in such a way that its electronic band structure is deeply modified: several 1 eV charge transfers have been measured, and noticeable hybridization of the graphene-π and metal-d orbitals were shown to disrupt the linear dispersion of the conduction band in graphene. The strong interaction between graphene and a Ni(111) substrate, inducing a magnetic moment of 0.05–0.1 μ_B, was invoked as the origin of X-ray magnetic

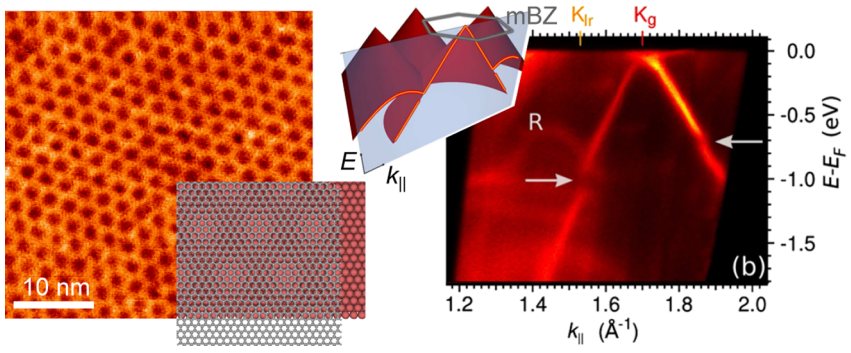

FIGURE 2. Scanning tunneling topograph of graphene on a 10 nm-thick Ir(111) thin film, revealing a moiré pattern, schematized with a ball-model in the inset (left panel). Electronic band structure of graphene below the Fermi level (E_F) for graphene/Ir(111), measured by angle-resolved photoemission spectroscopy, showing an almost intact Dirac cone, two minigaps and a replica band (R) (right panel, adapted in part from Pletikosic et al.[15] with permission, Copyright 2009 APS). The inset sketches a cut in an energy/wave-vector plane of the electronic band structure of graphene, around graphene's K point in the first Brillouin zone, together with three of the six replica cones arising from the moiré superpotential, whose apices are located at the corners of mini-Brillouin zone (mBZ).

circular dichroism.[10] With such at stake as all-carbon spintronics encompassing carbon spin transport channels and ferromagnetic carbon electrodes, the study of magnetism in carbon systems is a much debated issue, noticeably when it comes to the question of defect-induced magnetism. Epitaxial graphene–ferromagnetic systems offer an alternative route to the exploration of magnetism in two-dimensional (2D) carbon.

Graphene weakly interacts with some metals, for example, Pt, Cu, Au, Ag, or Ir. The electronic properties of graphene on Ir(111) were extensively studied recently because it was realized that this system is a model one for high-quality graphene,[11,12] which we also showed can be obtained on thin metal films[13] (Figure 2). Moreover, graphene is almost-free-standing[14] on this metal and preserves almost intact Dirac cones,[15] as we have shown with our collaborators. A faint charge transfer, resulting in 7×10^{-11} cm^{-2} hole-doped graphene, and a ca. 100 meV band gap at the Fermi level arising from hybridization of Ir(111) surface states with the π-bands of graphene were observed. Though weak, the interaction between graphene and this metal surface is not vanishing. Indeed the moiré between graphene and Ir(111), a superstructure formed due to the lattice mismatch between graphene and Ir(111), was found to be associated with a superpotential experienced by the electrons in graphene, giving rise to Dirac cone replicas and minigaps in the Dirac cones (Figure 2).

Graphene is inert and highly impermeable and thus functions as a capping layer preventing oxidation of the metal underneath. Oxidation-protected spin-polarization was reported with the help of graphene-capped Ni(111).[16] In this example, the strong interaction of graphene with Ni was found to mostly affect the topmost Ni layers, only slightly reducing the spin-polarization of the system. Very sensitive to perturbations are also the surface states of metals. On high-atomic-number metals, these surface states may be strongly spin-polarized, as it is the case on Ir(111). Graphene, unlike other layers that could be employed for protecting the surface from oxidation, only weakly interacts with Ir(111) and hence does not disrupt the delicate surface state.[17]

Intercalation provides advanced hybrid systems consisting of ultrathin films sandwiched between graphene and its metallic substrate.[18] Intercalation is believed to occur through defects, in a colander-like fashion, as we have shown recently by enabling intercalation at moderate temperature (below 600 K) in defected graphene.[19] Intercalation was shown to be an efficient means for tuning the graphene–substrate interaction. Accordingly graphene has been largely decoupled from a Ni substrate, for instance, by Au atomic layers.[20] Intercalation also allows new properties to be imparted to graphene. The Dirac cone of graphene was spin split, by 25 meV, with a Rashba effect due to the contact with a high-atomic-number element, Au.[20] A few recent works, including those with our collaborators, deal with intercalated graphene/metal systems displaying novel magnetic properties. We recently proved the preparation of Co films intercalated between graphene and Ir(111) via mild annealing and showed that the graphene/Co interface exhibits an unusually strong out-of-plane magnetic anisotropy.[19,21] As a result, the magnetization can be maintained perpendicular to the sample surface in Co films whose thickness exceeds 10 atomic layers, that is, thicker than most Co films sandwiched between two metallic layers. We foresee that the system is well-suited for spintronics

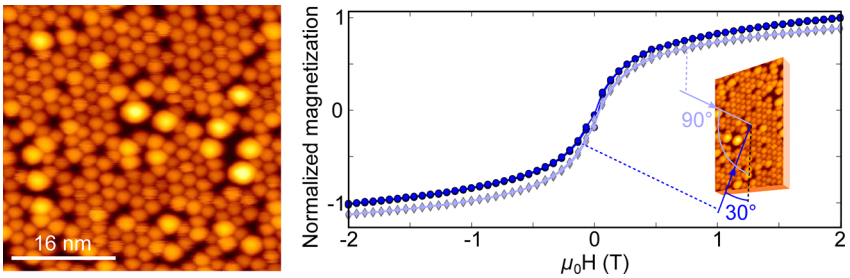

FIGURE 3. Scanning tunneling topograph (left) of Co clusters comprising 26 atoms on average and seeded by Pt clusters comprising 13 atoms on average, self-organized on the graphene/Ir(111) moiré. Normalized magnetization (M)−external magnetic field ($\mu_0 H$) loops (right) measured at 10 K for the same sample, with a grazing (30°) and a normal (90°) incidence X-ray beam.

applications in which the magnetization is manipulated, for instance, using laser illumination through the transparent graphene electrode or an external electric field applied through a gate dielectric layer deposited on top of the graphene protective barrier.

Moirés (Figure 2) are found on most graphene/metal systems. This pattern efficiently drives the organization of deposited metal atoms in 2D cluster lattices, with optimum order on graphene/Ir(111) at room temperature.[22,23] The recent discovery of a one-dimensional moiré in graphene/Fe(110)[24] holds promise for the preparation of nanowire lattices. In the case of Pt and Ir clusters on graphene/Ir(111), density functional calculations, supported by photoemission spectroscopy, indicate that rehybridization of the carbon atoms under the clusters stabilizes the system.[25,26] This new class of hybrid systems, where the nanocluster size is well-defined, opens the route to the size-dependent studies of the physical and chemical properties of graphene-supported clusters. Together with our collaborators, we started the study of the magnetic properties of Co-rich nanoclusters comprising a few tens of atoms and revealed unconventional isotropic superparamagnetism and difficult magnetization saturation (Figure 3), which point to a specific role of the cluster/graphene interface and raise the question of intercluster interactions.[27] Metallic clusters on graphene/Ir(111) were also employed for manipulating the electronic properties of graphene: a reduction of the charge carrier group velocity was induced by the cluster 2D lattice.[28]

3. Electronic Transport Properties of Graphene/Metal Dot Hybrids

The study of metal-on-graphene hybrid systems significantly differs from the symmetric case graphene-on-metal discussed in the previous section, because it allows testing of very different geometries and experimental situations involving metal clusters and isolated adatoms deposited on

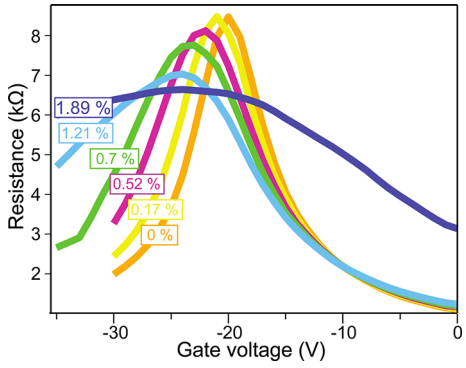

FIGURE 4. Electric field effect of a graphene transistor measured at 6 K in ultrahigh vacuum during evaporation of In at very low deposition rate. Field effect curves recorded *in situ*, exhibiting a maximum shifting to the left as the coverage increases up to 1.89% of a monolayer of In (courtesy of V. Sessi, ID08 beamline at ESRF, and A. Allain).

active graphene layers. For the reasons exposed above, only a weak bonding is expected when a metal adatom is coupled on graphene. The main effect that has been predicted[29] and observed[30] is a charge transfer between the metal and the graphene underlayer, without strong disruption of the π electron delocalization within graphene. This rather weak interaction is crucial for the electronic properties of hybrid devices because most of the outstanding properties of graphene (namely 2D gas of Dirac fermions with high mobility) are preserved. Depending on the difference of work function between the metal and carbon, a negative or positive shift of the Fermi level (i.e., electron or hole doping) is expected with respect to the Dirac point by up to 0.5 eV. An experimental example of metal decorated graphene is provided in Figure 4. It displays the evolution of the field-effect properties of a macroscopic graphene transistor (with an area of 10 mm^2) measured in ultrahigh vacuum during exposition to In vapor. The low temperature ensures that atoms are separated. The field effect is sensitive on very low coverage of In adatoms (less than 1% monolayer) showing a rigid shift of the charge neutrality point

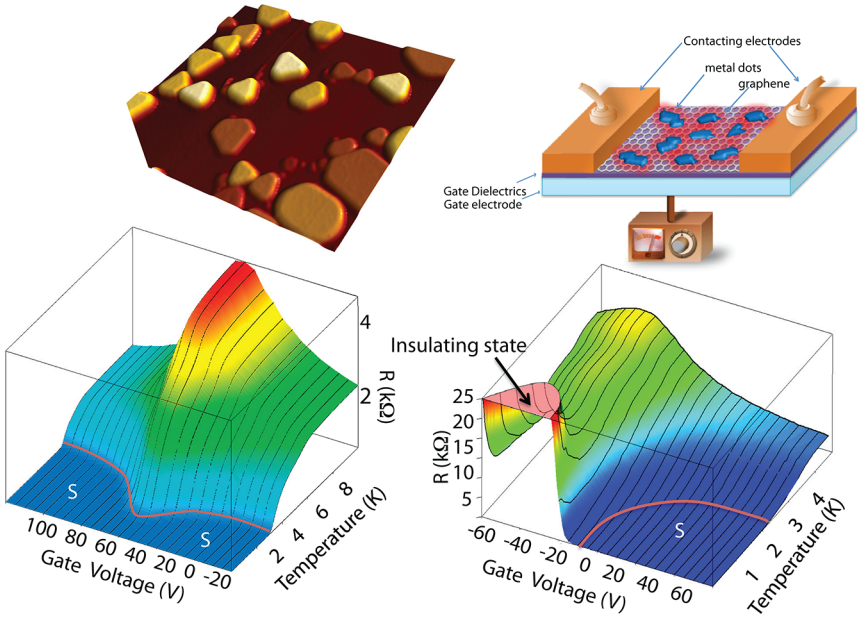

FIGURE 5. (top, left) Atomic force micrograph (scan size 1 μm) showing dewetted In islands on graphene. (top, right) Sketch of a typical graphene hybrid transistor device, in which the support is used as a backgate. Each cluster in the nonpercolating ensemble can be the source of correlated electrons in the surrounding graphene area (symbolized by a red halo). The electronic coupling between metal cluster islands can be tuned (tuning knob) with an electrostatic back-gate. (bottom, left and right) resistance of a graphene transistor, obtained by exfoliation of graphite (left) and chemical vapor deposition (right), decorated with 10 nm thick Sn clusters, as a function of the back-gate voltage (*X*-axis) and temperature (*Y*-axis). In the first case, the transistor transits toward a superconducting state with a gate tunable critical temperature (data taken from ref 38). The critical temperature is the lowest at the charge neutrality point. In the second case, superconductivity is observed far from the charge neutrality point, while gate-tuned transition toward a strongly insulating state is observed near the charge neutrality point, where the disordered graphene leads to a strongly insulating state (data adapted from ref 39).

(the gate value on which the transistor reaches its maximum of resistance). Upon larger deposition of In (typically several percent of a monolayer), the original electronic properties of graphene still remain intact, including similar conductance, bipolar field effect with carrier mobilities larger than 1000 $cm^2/(V\ s)$. The three main effects of the metal decoration are a shift in the charge neutrality point, a modest decrease in mobility, and a pronounced asymmetry between electron and hole transport. These effects are well described by inhomogeneous doping due to charge transfer from the metal islands to graphene[29] and have been reproduced with graphene coupled to other metals.[31] The charge induced by the metal reduces the mobility of both types of carriers via charged impurity scattering,[30] while the asymmetry in transport occurs because holes experience the pinned Fermi level under the In islands as a potential barrier, while electrons experience a potential well.[32,33]

Even more interesting than the influence of the metallic islands on the normal state properties of graphene is the effect of the electron correlations generated by an electronic order (superconductivity or magnetism), which can be transferred into the graphene by means of proximity effect. Graphene has indeed been shown to effectively preserve either superconducting[34] or spin-polarized currents[35] injected from contacting electrodes. The relative inertness of its exposed surface makes the superconducting proximity effect very efficient because the correlated electrons of the superconductor can effectively couple to the π electron cloud of graphene and generate superconducting correlations at distances exceeding several 100 nm.[34] To maintain electron coherence over larger distances (up to the entire graphene layer, which can reach meter scale) while retaining the unique 2D properties of the graphene sheet another strategy can be adopted: a large array of metal islands is placed in a nonpercolating network on top of the graphene sheet (see Figure 5, top right). The system does not anymore behave as a "metal–graphene–metal" one-dimensional junction but as 2D metal–graphene hybrid material. For that purpose, an array of metal nanodots needs to be deposited with a submicrometer pitch. Such a network can be achieved by self-assembly using the spontaneous dewetting of evaporated metallic thin films.

When evaporated on graphene at a controlled[36] temperature, low melting-point metals, such as the elemental superconductors Sn, In, or Pb, form clusters separated by bare graphene (Figure 5, top left).[37] Typically, a 10 nm

nominal thickness evaporated at room temperature yields a random array of Sn islands having typically 80 nm diameter and separated by 25 nm,[38,39] which will provide the functional devices discussed in the following.

The principle of such a device relies on the control of the superconducting proximity effect. Due to the delocalization of the π electronic state, nanoscaled sp^2 carbon materials are known to efficiently couple to superconducting metal electrodes[40] and to form tunable superconducting weak links. The quantum confinement of electron states in these systems results from the low-dimensionality of the crystalline carbon lattice. The confinement allows control of the effective superconducting coupling by adjusting the chemical potential of the nanostructure using an electrostatic gate. Beyond the practical interest of tuning the flow of a supercurrent, such a device allows testing of the limit of superconductivity at low dimensions.

In a superconductor-decorated graphene transistor (Figure 5, top right), the transition toward a global superconducting state results from the percolation of local superconductivity induced by the assembly of dots. Depending on the electronic disorder within the graphene layer, the superconductivity induced in the whole device exhibits different characteristics. In the case of low disorder (exfoliated) graphene, the device shows a transition toward a superconducting state at all gate voltages (see Figure 5, bottom left), typical[38] of a 2D superconductor (Berezinski–Kosterlitz–Thouless transition). If one uses a graphene layer with significant lattice disorder,[39] the 2D superconducting state cannot be preserved near the charge neutrality point, a regime in which an insulating state sets in (Figure 5, bottom right). By sweeping the gate voltage, a continuous transition from a superconducting to a truly insulating state can be induced. An intermediate metallic regime is also present at the transition showing sheet resistance on the order of the universal resistance quantum $R_Q = h/(4e^2)$. Such a hybrid system provides the first experimental proof of an electrostatically controlled superconducting to insulating transition based on proximity effect. This transition can be interpreted within the framework of granular superconductivity already observed in Josephson junction arrays.

As for superconductivity, the transfer of spin polarized currents and its detection through magnetoresistance were achieved in graphene hybrid transistors, when covered with ferromagnetic electrodes[35] or molecular nanomagnets.[41] At a smaller scale, graphene functionalized with ferromagnetic adatoms[42] is expected to provide model systems to study magnetic phase transition through Ruderman–Kittel–Kasuya–Yosida magnetic coupling. The epitaxial cluster/graphene/metal hybrids described in the previous section[27] may provide a playground for testing these predictions.

4. Optical Properties of Graphene Hybrids

Graphene presents unique optical properties: it absorbs only 2.3% of the incoming light over the whole visible range, while its spectral transparency can be gate-tuned.[43] It is foreseen as a transparent conductive electrode in flexible optoelectronics.[44] Graphene optical hybrids may be obtained with optically active nano-objects such as molecules, supramolecular architectures, semiconductor quantum dots, etc. The preparation of these hybrids may rely on simple nanoparticle deposition on graphene or on molecular coupling. The former approach allowed development of field effect phototransistors combining graphene and light-absorbing nanocrystals, exhibiting unprecedentedly high capacitively induced on/off ratio.[45] In the second approach, preserving graphene's unique electronic transport properties often requires noncovalent functionalization. In this view, molecules having aromatic groups such as aryl, phenyl, or pyrene ones offer the possibility for π-stacking functionalization to graphene.[46,47]

Strong fluorescence quenching of nearby nano-objects is observed on graphene,[48,49] up to distances reaching 300 Å from graphene. This proved valuable for optical localization of graphene flakes and molecule detection. Whether it originates from charge or energy transfer is not yet fully established.[50,51] Begliarbekov et al. demonstrated that the quenching is maximum at the Dirac point and follows the gate voltage-adjustable density of states of graphene.[52] Quenching luminescence with graphene allows better visibility to be obtained for other optical transitions such as the ones involved in Raman spectroscopy. Alkali-metal intercalated graphene exhibits sharp Raman features owing to this quench, but also because of the exaltation of the intramolecular electronic transition.[53] This phenomenon is related to a strong Raman signal enhancement, known as graphene-enhanced Raman spectroscopy (GERS), which we have recently investigated,[54] and originates from a chemical enhancement associated with charge transfer between a single molecule and graphene.[54,55] We have studied charge transfer theoretically[56] and put in evidence its prominent influence on the enhancement effect experimentally.[54] Moreover the GERS effect is not always present[57] and yet is strongly dependent on the molecule orientation on graphene.[58] This enhancement allow us to use Raman

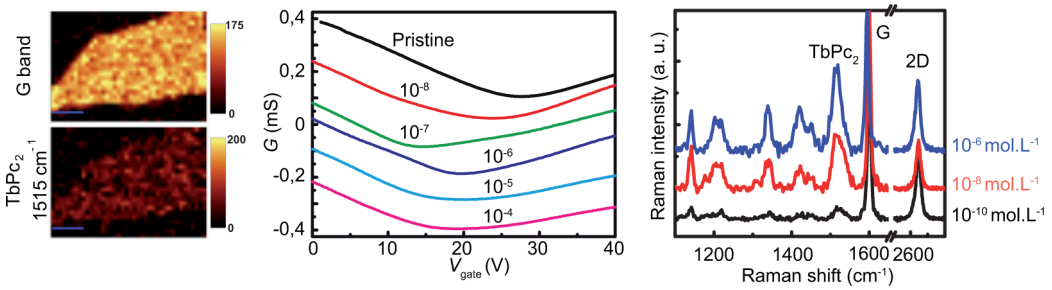

FIGURE 6. (Left) Raman intensity maps of graphene G mode (top) and phtalocyanin-based molecule mode detected after deposition from a 10^{-10} mol L^{-1} concentrated solution (bottom), scale bar is 4 μm and color scale is in CCD counts. (Middle) Transfer characteristics of a graphene transistor functionalized with different molecular concentrations. (Right) Raman spectra of the graphene device (red), the molecule (black), and the grafted system (blue). Adapted in part from ref 54 with permission. Copyright 2011 American Chemical Society.

spectroscopy as a sensitive detection technique, down to a few tens of molecules.[54] Figure 6 shows that charge transfer between molecules and graphene is detected both in the conductance and Raman signal from very low molecular concentration.

The GERS effect is optimum for the first molecular layer on graphene, as shown for porphyrin Langmuir–Blodgett films.[59] We found that the enhancement decreases dramatically with the number of graphene layers and saturates for thick molecular films, as expected for a charge-transfer-mediated phenomenon.[54] Interestingly, GERS can be modulated with an electrostatic back-gate, which provides a new degree of freedom, that is, by tuning the charge carrier density in graphene, which drives the coupling to the adsorbed molecules.[55]

Beyond the GERS effect, the Raman intensity can also be modulated by tailoring optical interferences in optical cavities. Interferences within graphene layers[60] and with the silicon oxide layer[61,62] strongly affect the graphene Raman signal, but also the one from adsorbed molecules. Ling and Zhang[59] demonstrated a modulation of the Raman signal intensity from phtalocyanin or porphyrin-based molecules when changing the silicon oxide thickness.[60] However this requires different samples. We implemented graphene in an optical cavity as a semitransparent mirror, which allowed us to tune the cavity with an electrostatic gate and hence to control interferences. This provides an integrated device combining optical interferences, GERS effect, and electromechanical coupling for promising active molecular platforms.[62]

5. Conclusion and Outlook

Graphene is an open platform onto which elements with specific properties (electronically ordered clusters, optically active adsorbates) can be deposited and possibly ordered using self-assembly, leading to functional hybrids. The easily accessible 2D electron gas in graphene provides an ideal playground on which to tune, via application of an electrostatic gate, the coupling between these elements. Charge carrier density-induced global electronic states and quantum phase transitions can accordingly be addressed in transport measurement. Epitaxy with metals yields another class of functional systems, some enriching the unique properties of graphene with new ones, such as spin-polarization or electronic band gaps, others exploiting graphene as a transparent conductive electrode acting on the electronic and magnetic properties of the material underneath thanks to strong interaction. We anticipate a wealth of functionalities to be achieved with the kind of hybrid systems discussed in this Account. Spintronics applications, making use of the long-lived electron spins in graphene or of graphene–ferromagnet stacks having novel magnetic properties, and catalytic clusters whose activity could be tuned by an electrostatic back-gate applied to a catalytically inert graphene support are a few illustrations.

We are grateful to our collaborators, C. Vo-Van, A. Kimouche, O. Fruchart, N. Rougemaille, T. Michely, A. T. N'Diaye, S. Schumacher, P. Ohresser, V. Sessi, N. Brookes, A. Schmid, A. Reserbat-Plantey, M. Lopes, R. Maurand, M. Urdampilletta, A. Candini, L. Bogani, W. Wernsdorfer, E. Bonet, C. Thirion, V. Reita, E. Eyraud, L. Del Rey, Nanofab team, Z. Han, A. Allain, H. Arjmandi-Tash, B. Kessler, C. Girit, A. Zettl, M. Saitta, P. Gava, G. Royal, and C. Bucher. We acknowledge financial support from ANR through the ANR-2010-BLAN-1019-NMGEM, ANR-Allucinan, and ANR-2010-BLAN-SUPERGRAPH contracts, the EC through the EU-NMP3-SL-2010-246073 GRENADA contract, and the ERC Advanced Grant MolNanoSpin No. 226558, the Alexander von Humboldt Foundation, C'Nano Rhône Alpes, and the Fondation Nanosciences.

BIOGRAPHICAL INFORMATION

Johann Coraux received his Ph.D. degree from Joseph Fourier University in 2006 after his work on the structural porperties of III-nitride quantum systems at CEA Grenoble. He then joined the group of Thomas Michely at the University of Cologne where he worked on epitaxial graphene as a Humboldt postdoctoral fellow in 2007 and 2008. He was appointed a researcher position at CNRS in 2008 at Institut Néel in Grenoble where he works on the preparation and study of the properties of epitaxial graphene hybrid systems.

Laëtitia Marty investigated carbon nanotube transistors under the supervision of Anne Marie Bonnot and Vincent Bouchiat during her Ph.D. at LEPES-CNRS Grenoble (2001−2004). She then joined the group of Richard Martel as a postdoctoral fellow, University of Montreal (2004−2006). In 2006, she took a researcher position at Institut Néel-CNRS Grenoble to focus on nanotube and graphene/molecule hybrids.

Nedjma Bendiab conducted her Ph.D. on doped carbon nanotubes from 2000 to 2003 under the supervision of Jean-Louis Sauvajol and Robert Almairac at Montpellier University. She then joined the group of Alfonso San Miguel at Lyon University as a postdoctoral fellow, working on sp^2 carbon under high pressure and temperature. She was Assistant Professor at Pierre et Marie Curie University in Paris from 2004 to 2006. She is now appointed to Grenoble Joseph Fourier University and works on the electromechanical properties of graphene and nanotube devices.

Vincent Bouchiat did his Ph.D. at CEA-Saclay from 1993 to 1997 on quantum transport in superconducting devices under the supervision of Michel Devoret. He was appointed to a researcher position at CNRS in 1997 at the University of Marseilles designing quantum devices using scanning probe microscopy. Since 2000, he has been part of CNRS-Grenoble and works on electron transport properties of carbon nanostructures. He was a visiting scholar at UC Berkeley in 2007−2009, collaborating on various projects involving graphene nanodevices.

FOOTNOTES

*To whom correspondence should be addressed. E-mail: johann.coraux@grenoble.cnrs.fr.
The authors declare no competing financial interest.

REFERENCES

1 LeBaron, P.; Wang, Z.; Pinnavaia, T. Polymer-layered silicate nanocomposites: An overview. *Appl. Clay Sci.* **1999**, *15*, 11–29.

2 Giannelis, E. Polymer layered silicate nanocomposites. *Adv. Mater.* **1996**, *8*, 29–35.

3 Bruce, P.; Scrosati, B.; Tarascon, J. Nanomaterials for rechargeable lithium batteries. *Angew. Chem., Int. Ed.* **2008**, *47*, 2930–2946.

4 Korneva, G.; Ye, H.; Gogotsi, Y.; Halverson, D.; Friedman, G.; Bradley, J.; Kornev, K. Carbon nanotubes loaded with magnetic particles. *Nano Lett.* **2005**, *5*, 879–884.

5 Xu, Y.; Liu, Z.; Zhang, X.; Wang, Y.; Tian, J.; Huang, Y.; Ma, Y.; Zhang, X.; Chen, Y. A graphene hybrid material covalently functionalized with porphyrin: Synthesis and optical limiting property. *Adv. Mater.* **2009**, *21*, 1275–1279.

6 Yang, X.; Zhang, X.; Ma, Y.; Huang, Y.; Chen, Y. Superparamagnetic graphene oxide-Fe_3O_4 nanoparticles hybrid for controlled targeted drug carriers. *J. Mater. Chem.* **2009**, *19*, 2710–2714.

7 Wang, D.; Choi, D.; Li, J.; Yang, Z.; Nie, Z.; Kou, R.; Hu, D.; Wang, C.; Saraf, L. V.; Zhang, J.; Aksay, I. A.; Liu, J. Self-assembled TiO_2−graphene hybrid nanostructures for enhanced Li-ion insertion. *ACS Nano* **2009**, *3*, 907–914.

8 Liang, Y.; Li, Y.; Wang, H.; Zhou, J.; Wang, J.; Regier, T.; Dai, H. Co_3O_4 nanocrystals on graphene as a synergistic catalyst for oxygen reduction reaction. *Nat. Mater.* **2011**, *10*, 780–786.

9 Batzill, M. The surface science of graphene: Metal interfaces, CVD synthesis, nanoribbons, chemical modifications, and defects. *Surf. Sci. Rep.* **2012**, *67*, 83–115.

10 Weser, M.; Rehder, Y.; Horn, K.; Sicot, M.; Fonin, M.; Preobrajenski, A. B.; Voloshina, E. N.; Goering, E.; Dedkov, Y. S. Induced magnetism of carbon atoms at the graphene/Ni(111) interface. *Appl. Phys. Lett.* **2010**, *96*, No. 012504.

11 Coraux, J.; Busse, C.; Michely, T. Structural coherency of graphene on Ir (111). *Nano Lett.* **2008**, *8*, 565–570.

12 Coraux, J.; N'Diaye, A. T.; Busse, C.; Michely, T. Epitaxial growth of graphene on single-crystalline metal surfaces. In *Thin film growth − Physics, materials science and applications*; Zexian, C., Ed.; Woodhead Publishing: Oxford−Cambridge−Philadelphia−New Delhi, 2011.

13 Vo-Van, C.; Kimouche, A.; Reserbat-Plantey, A.; Fruchart, O.; Bayler-Guillemaud, P.; Bendiab, N.; Coraux, J. Epitaxial graphene prepared by chemical vapor deposition on single crystal thin iridium films on sapphire. *Appl. Phys. Lett.* **2011**, *98*, No. 181903.

14 Busse, C.; Lazic, P.; Djemour, R.; Coraux, J.; Gerber, T.; Atodiresei, N.; Caciuc, V.; Brako, R.; Diaye, A. T. N.; Blugel, S.; Zegenhagen, J.; Michely, T. Graphene on Ir(111): Physisorption with chemical modulation. *Phys. Rev. Lett.* **2011**, *107*, No. 036101.

15 Pletikosic, I.; Kralj, M.; Pervan, P.; Brako, R.; Coraux, J.; N'Diaye, A.; Busse, C.; Michely, T. Dirac cones and minigaps for graphene on Ir(111). *Phys. Rev. Lett.* **2009**, *102*, No. 056808.

16 Dedkov, Y. S.; Fonin, M.; Laubschat, C. A possible source of spin-polarized electrons: The inert graphene/Ni(111) system. *Appl. Phys. Lett.* **2008**, *92*, No. 052506.

17 Varykhalov, A.; Marchenko, D.; Scholz, M. R.; Rienks, E. D. L.; Kim, T. K.; Bihlmayer, G.; Sánchez-Barriga, J.; Rader, O. Ir(111) surface state with giant Rashba splitting persists under graphene in air. *Phys. Rev. Lett.* **2012**, *108*, No. 066804.

18 Tontegode, A. Y. Carbon on transition metal surfaces. *Prog. Surf. Sci.* **1991**, *38*, 201–429.

19 Coraux, J.; N'Diaye, A. T.; Rougemaille, N.; Vo-Van, C.; Kimouche, A.; Yang, H.-X.; Chshiev, M.; Bendiab, N.; Fruchart, O.; Schmid, A. K. Air-protected epitaxial graphene/ferromagnet hybrids prepared by chemical vapor deposition and intercalation. *J. Phys. Chem. Lett.* **2012**, *3*, 2059–2063.

20 Varykhalov, A.; Sánchez-Barriga, J.; Shikin, A.; Biswas, C.; Vescovo, E.; Rybkin, A.; Marchenko, D.; Rader, O. Electronic and magnetic properties of quasifreestanding graphene on Ni. *Phys. Rev. Lett.* **2008**, *101*, No. 157601.

21 Rougemaille, N.; N'Diaye, A. T.; Coraux, J.; Vo-Van, C.; Fruchart, O.; Schmid, A. K. Perpendicular magnetic anisotropy of cobalt films intercalated under graphene. *Appl. Phys. Lett.* **2012**, *101*, No. 142403.

22 N'Diaye, A.; Bleikamp, S.; Feibelman, P.; Michely, T. Two-dimensional Ir cluster lattice on a graphene moire on Ir (111). *Phys. Rev. Lett.* **2006**, *97*, No. 215501.

23 N'Diaye, A. T.; Gerber, T.; Busse, M.; Myslivecek, J.; Coraux, J.; Michely, T. A versatile fabrication method for cluster superlattices. *New J. Phys.* **2009**, *11*, No. 103045.

24 Vinogradov, N. A.; Zakharov, A. A.; Kocevski, V.; Rusz, J.; Simonov, K. A.; Eriksson, O.; Mikkelsen, A.; Lundgren, E.; Vinogradov, A. S.; Martensson, N.; Preobrajenski, A. B. Formation and structure of graphene waves on Fe(110). *Phys. Rev. Lett.* **2012**, *109*, No. 026101.

25 Feibelman, P. Pinning of graphene to Ir(111) by flat Ir dots. *Phys. Rev. B* **2008**, *77*, No. 165419.

26 Knudsen, J.; Feibelman, P.; Gerber, T.; Granäs, E.; Schulte, K.; Stratmann, P.; Andersen, J.; Michely, T. Clusters binding to the graphene moiré on Ir(111): X-ray photoemission compared to density functional calculations. *Phys. Rev. B* **2012**, *85*, No. 035407.

27 Vo-Van, C.; Schumacher, S.; Coraux, J.; Sessi, V.; Fruchart, O.; Brookes, N. B.; Orhesser, P.; Michely, T. Magnetism of cobalt nanoclusters on graphene on iridium. *Appl. Phys. Lett.* **2011**, *99*, No. 142504.

28 Rusponi, S.; Papagno, M.; Moras, P.; Vlaic, S.; Etzkorn, M.; Sheverdyaeva, P.; Pacilé, D.; Brune, H.; Carbone, C. Highly anisotropic Dirac cones in epitaxial graphene modulated by an island superlattice. *Phys. Rev. Lett.* **2010**, *105*, No. 246803.

29 Giovannetti, G.; Khomyakov, P. A.; Brocks, G.; Karpan, V. M.; van den Brink, J.; Kelly, P. J. Doping graphene with metal contacts. *Phys. Rev. Lett.* **2008**, *101*, No. 026803.

30 Pi, K.; McCreary, K. M.; Bao, W.; Han, W.; Chiang, Y. F.; Li, Y.; Tsai, S.-W.; Lau, C. N.; Kawakami, R. K. Electronic doping and scattering by transition metals on graphene. *Phys. Rev. B* **2009**, *80*, No. 075406.

31 H., L. J.; Balasubramanian, K.; Weitz, R.; Burghard, M.; Kern, K. Contact and edge effects in graphene devices. *Nat. Nanotechnol.* **2008**, *3*, 486–490.

32 Farmer, D. B.; Golizadeh-Mojarad, R.; Perebeinos, V.; Lin, Y.-M.; Tulevski, G. S.; Tsang, J. C.; Avouris, P. Chemical doping and electron hole conduction asymmetry in graphene devices. *Nano Lett.* **2009**, *9*, 388–392.

33 Huard, B.; Stander, N.; Sulpizio, J. A.; Goldhaber-Gordon, D. Evidence of the role of contacts on the observed electron-hole asymmetry in graphene. *Phys. Rev. B* **2008**, *78*, No. 121402.

34 Heersche, H.; Jarillo-Herrero, P.; Oostinga, J.; Vandersypen, L.; Morpurgo, A. Bipolar supercurrent in graphene. *Nature* **2007**, *446*, 56–59.

35 Tombros, N.; Jozsa, C.; Popinciuc, M.; Jonkman, H.; van Wees, B. Electronic spin transport and spin precession in single graphene layers at room temperature. *Nature* **2007**, *448*, 571–574.

36 Zayed, M.; Elsayed-Ali, H. Melting behavior of as-deposited and recrystallized indium nanocrystals. *Thin Solid Films* **2005**, *489*, 42–49.

37 Heyraud, J.; Métois, J. Equilibrium shape and temperature; Lead on graphite. *Surf. Sci.* **1983**, *128*, 334–342.

38 Kessler, B. M.; Girit, i. m. c. O.; Zettl, A.; Bouchiat, V. Tunable superconducting phase transition in metal-decorated graphene sheets. *Phys. Rev. Lett.* **2010**, *104*, No. 047001.

39 Allain, A.; Han, Z.; Bouchiat, V. Electrical control of the superconducting-to-insulating transition in graphene/metal hybrids. *Nat. Mater.* **2012**, *11*, 590–594.

40 Bouchiat, V. Superconducting Weak-links made of Carbon Nanostructures. In *Nanoelectronics and Nanophotonics*; Sattler, K. D., Ed.; Handbook of Nanophysics, Vol. 6, Taylor & Francis (CRC Press): London, 2010, Chapter 7.

41 Candini, A.; Klyatskaya, S.; Ruben, M.; Wernsdorfer, W.; Affronte, M. Graphene spintronic devices with molecular nanomagnets. *Nano Lett.* **2011**, *11*, 2634–2639.

42 Wang, Y.; Cheng, H.-P. Interedge magnetic coupling in transition-metal terminated graphene nanoribbons. *Phys. Rev. B* **2011**, *83*, No. 113402.

43 Liu, M.; Yin, X.; Ulin-Avila, E.; Geng, B.; Zentgraf, T.; Ju, L.; Wang, F.; Zhang, X. A. Graphene-based broadband optical modulator. *Nature* **2011**, *474*, 64–67.

44 Bonaccorso, F.; Sun, Z.; Hasan, T.; Ferrari, A. C. Graphene photonics and optoelectronics. *Nat. Photonics* **2010**, *4*, 611.

45 Konstantatos, G.; Badioli, M.; Gaudreau, L.; Osmond, J.; Bernechea, M.; de Arquer, F.; Gatti, F.; Koppens, F. Hybrid graphene-quantum dot phototransistors with ultrahigh gain. *Nat. Nanotechnol.* **2012**, *7*, 363–368.

46 Su, Q.; Pang, S.; Alijani, V.; Li, C.; Feng, X.; Müllen, K. Composites of graphene with large aromatic molecules. *Adv. Mater.* **2009**, *21*, 3191–3195.

47 Kamat, P. V. Graphene-based nanoassemblies for energy conversion. *J. Phys. Chem. Lett.* **2011**, *2*, 242–251.

48 Swathi, R. S.; Sebastian, K. L. Long range resonance energy transfer from a dye molecule to graphene has (distance)(-4) dependence. *J. Chem. Phys.* **2009**, *130*, No. 086101.

49 Chen, Z.; Berciaud, S.; Nuckolls, C.; Heinz, T. F.; Brus, L. E. Energy transfer from individual semiconductor nanocrystals to graphene. *ACS Nano* **2010**, *4*, 2964–2968.

50 Ramakrishna Matte, H.; Subrahmanyam, K.; Venkata Rao, K.; George, S. J.; Rao, C. Quenching of fluorescence of aromatic molecules by graphene due to electron transfer. *Chem. Phys. Lett.* **2011**, *506*, 260–264.

51 Kasry, A.; Afzali-Ardakani, A.; Tulevski, G. Highly efficient fluorescence quenching with graphene. *J. Phys. Chem. C* **2012**, *116*, 2858–2862.

52 Begliarbekov, M.; Sul, O.; Santanello, J.; Ai, N.; Zhang, X.; Yang, E.-H.; Strauf, S. Localized States and resultant band bending in graphene antidot superlattices. *Nano Lett.* **2011**, *11*, 1254–1258.

53 Jung, N.; Crowther, A. C.; Kim, N.; Kim, P.; Brus, L. Raman enhancement on graphene: Adsorbed and intercalated molecular species. *ACS Nano* **2010**, *4*, 7005–7013.

54 Lopes, M.; Candini, A.; Urdampilleta, M.; Reserbat-Plantey, A.; Bellini, V.; Klyatskaya, S.; Marty, L.; Ruben, M.; Affronte, M.; Wernsdorfer, W.; Bendiab, N. Surface-enhanced Raman signal for terbium single-molecule magnets grafted on graphene. *ACS Nano* **2010**, *4*, 7531–7537.

55 Xu, H.; Chen, Y.; Xu, W.; Zhang, H.; Kong, J.; Dresselhaus, M. S.; Zhang, J. Modulating the charge-transfer enhancement in GERS using an electrical field under vacuum and an n/p-doping atmosphere. *Small* **2011**, *7*, 2945–2952.

56 Reserbat-Plantey, A.; Gava, P.; Bendiab, N.; Saitta, A. M. First-principles study of an iron-based molecule grafted on graphene. *Europhys. Lett.* **2011**, *96*, No. 57001.

57 Thrall, E. S.; Crowther, A. C.; Yu, Z.; Brus, L. E. R6G on graphene: High Raman detection sensitivity, yet decreased Raman cross-section. *Nano Lett.* **2012**, *12*, 1571–1577.

58 Ling, X.; Wu, J.; Xu, W.; Zhang, J. Probing the effect of molecular orientation on the intensity of chemical enhancement using graphene-enhanced Raman spectroscopy. *Small* **2012**, *8*, 1365–1372.

59 Ling, X.; Zhang, J. First-layer effect in graphene-enhanced Raman scattering. *Small* **2010**, *6*, 2020–2025.

60 Wang, Y. Y.; Ni, Z. H.; Shen, Z. X.; Wang, H. M.; Wu, Y. H. Interference enhancement of Raman signal of graphene. *Appl. Phys. Lett.* **2008**, *92*, No. 043121.

61 Ling, X.; Xie, L.; Fang, Y.; Xu, H.; Zhang, H.; Kong, J.; Dresselhaus, M. S.; Zhang, J.; Liu, Z. Can graphene be used as a substrate for Raman enhancement? *Nano Lett.* **2010**, *10*, 553–561.

62 Reserbat-Plantey, A.; Marty, L.; Arcizet, O.; Bendiab, N.; Bouchiat, V. A local optical probe for measuring motion and stress in a nanoelectromechanical system. *Nat. Nanotechnol.* **2012**, *7*, 151–155.